Hunting squarks in Higgsino LSP scenarios at the LHC

Ernesto Arganda[®], ^{1,2,*} Antonio Delgado[®], ^{3,†} Roberto A. Morales[®], ^{2,‡} and Mariano Quirós^{4,§}

¹Instituto de Física Teórica UAM-CSIC, C/Nicolás Cabrera 13-15,

Campus de Cantoblanco, 28049 Madrid, Spain

²IFLP, CONICET—Departamento de Física, Universidad Nacional de La Plata,

C.C. 67, 1900 La Plata, Argentina

³Department of Physics, University of Notre Dame, 225 Nieuwland Hall Notre Dame, Indiana 46556, USA

⁴Institut de Física d'Altes Energies (IFAE) and BIST, Campus UAB, 08193 Bellaterra, Barcelona, Spain

(Received 3 January 2022; accepted 12 January 2023; published 26 January 2023)

Current searches for squarks are inefficient in cases when the squark does not directly decay to the lightest supersymmetric particle (LSP), because those decays are Yukawa suppressed. This occurs when producing the first two generations of squarks and when, at the same time, there are several electroweakinos lighter than those squarks. In this paper, we analyze the signal of the pair production of squarks that subsequently decay to an intermediate neutralino ($\tilde{\chi}_3^0$) plus jets. The neutralino will then decay to the LSP (mainly Higgsino) and a Higgs. We have simulated the events and designed a discovery strategy based on a signal of two jets, four *b* quarks, and missing transverse energy. We obtain very promising values for the Large Hadron Collider sensitivity at 14 TeV and 300 fb⁻¹.

DOI: 10.1103/PhysRevD.107.015024

I. INTRODUCTION

Supersymmetry (SUSY) is one of the prime scenarios for physics beyond the Standard Model (SM). It can achieve a solution to the big hierarchy problem, accommodate gauge coupling unification, and, if one assumes R-parity conservation, produce a candidate for dark matter. One of the consequences of R-parity conservation is that the lightest supersymmetric particle (LSP) is neutral and stable at the cosmological level, which means a lot of missing transverse energy (MET) on cascade decays at the Large Hadron Collider (LHC). In particular, the minimal supersymmetric SM extension (MSSM) is, at present, the subject of extensive experimental searches at the LHC, mainly concerning gauginos, Higgsinos (the supersymmetric partners of gauge and Higgs bosons), squarks, and sleptons (the supersymmetric partners of quarks and leptons).

In the MSSM, the gaugino sector contains, on top of the gluino (a Majorana fermion), the electroweak neutralinos (four Majorana fermions $\tilde{\chi}_i^0$, i = 1, ...4, an admixture of the

Published by the American Physical Society under the terms of the Creative Commons Attribution 4.0 International license. Further distribution of this work must maintain attribution to the author(s) and the published article's title, journal citation, and DOI. Funded by SCOAP³. bino, the neutral wino, and the two neutral Higgsinos) and charginos (two Dirac fermions $\tilde{\chi}_a^{\pm}$, a=1, 2, an admixture of the two charged winos and the two charged Higgsinos). The mass matrices for the neutralino and chargino sectors only depend, leaving aside the electroweak breaking parameters in the MSSM (v and $\tan \beta$), on three mass parameters: the soft breaking masses for binos (M_1) and winos (M_2) and the supersymmetric Higgsino mass (μ) . In view of the above comments, it should be clear that the neutralino sector is pretty much independent of the particular mechanism of SUSY breaking in the scalar sector, as well as the subsequently induced electroweak breaking. Moreover, in R-parity-conserving scenarios, the neutralino sector is an excellent candidate to accommodate the LSP (i.e., $\tilde{\chi}_1^0$), which makes experimental SUSY searches with a lot of MET as model independent as possible. In this paper, we will assume that the LSP is the lightest neutralino, and is usually a Higgsino, thus easily avoiding cosmological problems.

However, in most experimental analyses, it is further assumed that the LSP $(\tilde{\chi}_1^0)$ is an isolated neutral state, and squark searches assume 100% branching ratios (BR) to $\tilde{\chi}_1^0$ plus jet. This scenario is only possible, for neutralino masses larger than the electroweak scale, if the neutralino LSP is mostly bino. That assumption can have problems when one makes dark matter considerations, as the bino tends to overclose the Universe [1]. If, on the other hand, one assumes that the Higgsino is lighter than the bino and the wino, since the Higgsino is an SU(2) doublet, one has a neutral state as the LSP $(\tilde{\chi}_1^0)$ and a charged and a neutral

^{*}ernesto.arganda@csic.es

adelgad2@nd.edu

roberto.morales@fisica.unlp.edu.ar

quiros@ifae.es

one $(\tilde{\chi}_1^+, \tilde{\chi}_2^0)$ very close in mass. In this case, the Higgsino has no cosmological problems for masses below 1.1 TeV (but it only accounts for all the relic abundance for a mass of 1.1 TeV; for lower masses, one needs other components for DM) and, if there are no other electroweakinos with masses below the squark masses, the experimental signature is captured in current analyses that assume a 100% BR to the LSP. Then, even though there may be decays from squarks to the other two light electroweakinos $(\tilde{\chi}_1^+, \tilde{\chi}_2^0)$, subsequent decays of these electroweakinos will lead to the same signal, since any of their decay products will be very soft.

A far more interesting situation, which we will consider in this paper, occurs when there is an intermediate neutral state $(\tilde{\chi}_3^0)$ between the squarks and the LSP (and associated states). This situation happens when there is a small hierarchy between the masses $(\mu < M_1 < M_{\tilde{q}} < M_2)$: i.e., the Higgsino is lighter than the bino, which in turn is lighter than the squarks, while the wino is essentially decoupled. This spectrum with $\tilde{\chi}_3^0$ lighter than strongly interacting sparticles was previously analyzed for the case of gluino production [2,3], and also for the case of stop-pair production [4]. This kind of spectrum escapes current experimental searches because the experimental cuts are very inefficient for this particular signal.

In this paper, we are interested in decays of squarks within the MSSM for the case of Higgsinos being the LSP, much heavier winos, and first- and second-generation squarks at an intermediate scale between those of the bino and wino masses. We then assume the decay channel $\tilde{q} \rightarrow \tilde{\chi}_3^0 j$ and prevent the direct decay into the LSP by assuming third-generation squarks, which would decay into the LSP by the Yukawa interaction, to be heavier than first- and second-generation ones. The assumption that the third-generations squarks are heavier than those of the first two generations, a hierarchy which appears naturally in the quark and lepton sectors in the SM, can be theoretically implemented in the effective theory of superstring models [5], where the sfermion soft masses do depend on the corresponding modular weights.

The paper is structured as follows: In Sec. II, we present a search strategy for this class of experimental signature at the LHC, characterizing the signal against the background. Section III is devoted to the analysis of the corresponding LHC sensitivity, by means of our search strategy, within the masses of the bino and squark parameter space. We finally conclude with a brief discussion of the main results in Sec. IV. The details of the benchmark point considered in this work are summarized in the Appendix.

II. SQUARK-PAIR PRODUCTION AT THE LHC: COLLIDER STUDY

Within the MSSM Higgsino LSP scenarios presented above, the proposed experimental LHC signature originates

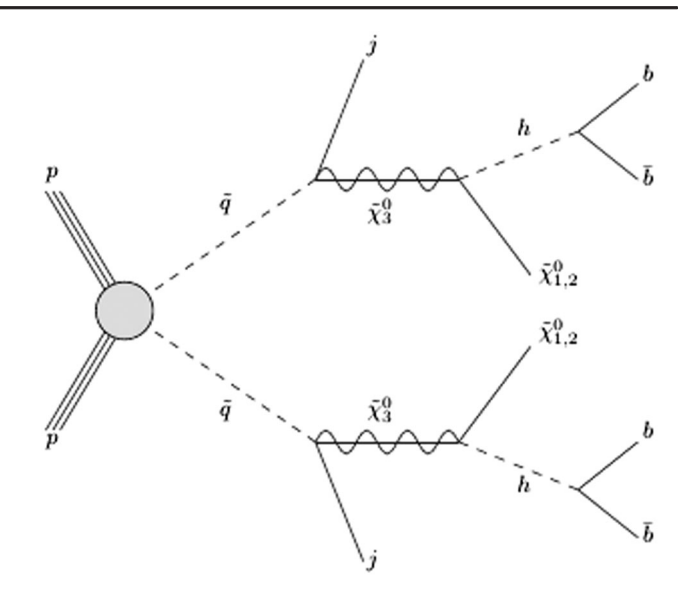


FIG. 1. Relevant SUSY process corresponding to squark production with $2j + 4b + E_T^{\text{miss}}$ in the final state.

from the squark-pair production, $pp o \tilde{q}\tilde{q}^*$, that decays into $\tilde{\chi}_3^0$ (essentially a bino) and one light jet $(\tilde{q} o \tilde{\chi}_3^0 j)$. Each $\tilde{\chi}_3^0$ decays then into the LSP $(\tilde{\chi}_1^0)$ and h, the lightest MSSM Higgs boson considered here as the 125 GeV Higgs boson, which in turn decays into a b-quark pair. Thus, the LHC signature is made of two light jets, four b jets, and a lot of missing transverse energy $(2j+4b+E_T^{\rm miss})$, as shown in Fig. 1. The main backgrounds are separated into the following categories: QCD multijet; $t\bar{t}$ production; $t\bar{t}$ production associated with electroweak or Higgs bosons, $t\bar{t}+X$ $(X=W,Z,\gamma^*,h)$; $Z+{\rm jets}$ and $W+{\rm jets}$ productions; and diboson production $(WW,ZZ,WZ,Wh,{\rm and}~Zh)$ plus jets.

Our LHC search strategy is developed for a center-of-mass energy of $\sqrt{s} = 14$ TeV and an integrated luminosity of $\mathcal{L} = 1$ ab⁻¹, corresponding to the high-luminosity LHC (HL-LHC) stage. MadGraph_aMC@NLO 2.8.1 [6] is used for the Monte Carlo generation of the signal and the main backgrounds; the parton showering and hadronization are obtained with PYTHIA 8.2 [7], and the detector response is simulated with Delphes 3.3.3 [8].

On the other hand, we have confronted our spectrum of interest with the general searches at the LHC of new physics for 13 TeV by using the software CheckMATE 2.0.24 [9], and we conclude that the spectrum is allowed by the validated analyses. For each validated search, the ratio of the resulting signal events and the 95% C.L. limits on the signal is computed, and the r parameter is the maximum of these ratios. In particular, the resulting r parameters are below 0.1, with the search (Ref. [10]) in the SRI - MLL - 60 region carrying the most weight. From this comparison, the general validated searches in CheckMATE are far from being sensitive to squark-pair production with our

spectrum, so that it is relevant to develop a dedicated search strategy for the signature considered here. Notice that as the r-parameter values are too low, we do not expect that the current experimental analysis for $\mathcal{L} = 1000 \text{ fb}^{-1}$ will exclude our spectrum. More recent experimental searches—see, for instance, Refs. [11,12]—have similar signatures to ours, although they are not dedicated to our spectrum, since there are no squarks as intermediate states. We will see that our most optimistic observed number of signal events for $\mathcal{L} = 137 \text{ fb}^{-1}$ is ~ 2 (see our Table IV), and this value is roughly inside the uncertainties of the

$$p_T^{j_1} > 180 \text{ GeV}, \qquad p_T^{j_2} > 140 \text{ GeV}, \qquad p_T^{j_3} > 70 \text{ GeV}, \qquad p_T^{j_4} > 35 \text{ GeV},$$
 $p_T^{b_1} > 90 \text{ GeV}, \qquad p_T^{b_2} > 20 \text{ GeV}, \qquad p_T^{b_3} > 20 \text{ GeV}, \qquad p_T^{b_4} > 20 \text{ GeV},$

with j_1 (b_1) being the most energetic light (b) jet, and j_4 (b_4) the least energetic one. The MLM algorithm [13,14] has been implemented for jet matching and merging. With the intention of optimizing the event simulation and checking that the jet distributions are smooth, xqcut is chosen to be 20 GeV for all generated samples, and qcut is equal to 30, 50, and 250 GeV for backgrounds with vector bosons, $t\bar{t}$, and signal, respectively. These parameters in the run and PYTHIA cards represent the minimum k_T jet measure between partons. A working point for the efficiency of b tagging of 0.75 is used, with a rate of misidentification of 0.01 for light jets and 0.1 for c jets (internal analysis codes and simulation input files are available upon request to authors).

It is appropriate to make the following comments on the signal and its corresponding backgrounds:

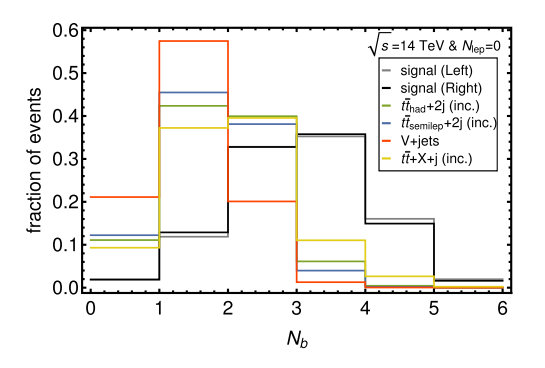
(1) Signal. Supersymmetric spectrum and decay rates for the signal have been calculated with SOFTSUSY.4.1.10 [15–21], while the production cross section of a pair of squarks is obtained from Ref. [22]. We consider two cases: the *Left* case, for $\tilde{u}_L \tilde{u}_L$ and $\tilde{d}_L \tilde{d}_L$ productions, and the *Right* case, for $\tilde{u}_R \tilde{u}_R$ production. In both cases, we keep the LSP mass almost fixed around 500 GeV, and we scan over the parameter space $M_{\tilde{q}} \in$ [800, 1100] GeV and $M_{\tilde{\chi}_{3}^{0}} \in [600, 900]$ GeV. In these parameter space regions, for the Left case, we have $\tilde{q}_L \tilde{q}_L$ production cross sections in the range [45, 160] fb and BR($\tilde{q}_L \to q\tilde{\chi}_3^0$) \in [0.19, 0.88]. On the other hand, for the *Right* case, we have $\sigma(pp \rightarrow$ $\tilde{u}_R \tilde{u}_R) \in [58, 400] \text{ fb}$ and $BR(\tilde{u}_R \to u\tilde{\chi}_3^0) \in$ [0.56, 0.95]. See the Appendix for more details. However, production cross sections for $pp \rightarrow d_R d_R$ are typically 1 order of magnitude smaller than $\tilde{q}_L \tilde{q}_L$ results in Refs. [11,12]. Then these similar searches do not exclude our spectrum.

For the simulation of the signal, the default cuts on the transverse momenta of the light jets and b jets are used $(p_T^J > 20 \text{ GeV} \text{ and } p_T^b > 20 \text{ GeV})$. However, in order to decrease the large background cross sections and make event generation more efficient, the generator-level cuts of Eq. (1), on the p_T of the light jets and b jets, are imposed for the background simulation, since very energetic b jets and light jets from the decays of Higgs bosons and squarks are expected, respectively:

$$p_T^{j_3} > 70 \text{ GeV}, \qquad p_T^{j_4} > 35 \text{ GeV},$$

 $p_T^{b_3} > 20 \text{ GeV}, \qquad p_T^{b_4} > 20 \text{ GeV},$ (1)

- and $\tilde{u}_R \tilde{u}_R$ cases, and we will not take this process into account (see, for instance, Ref. [23]).
- (2) QCD multijet background. It is commonly treated using data-driven techniques and is intractable with our computational capacity. An estimate of this background by recasting the analysis in Ref. [24] is included, in which a similar cut-based analysis is performed for a similar experimental signature. In particular, as our signal is expected to have a large amount of E_T^{miss} , variables related to this observable, such as the E_T^{miss} significance, will substantially decrease this class of background with nongenuine missing transverse energy. Moreover, the characteristic \vec{p}_T^{miss} spatial configuration can be used for reducing this background.
- (3) tt production. Its fully hadronic and semileptonic decay channels are included. The branching fraction of the fully hadronic channel is 0.457, while that of the semileptonic is 0.438. After applying the cuts of Eq. (1), one expects 1.36×10^6 events for the fully hadronic channel and 0.42×10^6 events for the semileptonic one. To be somewhat more realistic with the simulation of this background, we consider an extra jet, which translates to 0.83×10^6 and 0.25×10^6 more events for the fully hadronic and semileptonic channels, respectively. An estimate of $t\bar{t} + 2i$ is also included through an extra factor of 10% for the simulated events of $t\bar{t}$ plus $t\bar{t} + j$ (this 10% comes from the ratio of the corresponding cross
- (4) $t\bar{t} + X$ production. In relation to $t\bar{t}$, the extra boson generates a genuine source of E_T^{miss} (more b jets) for the hadronic (semileptonic) top-quark pair. $t\bar{t}_{\text{semilep}}+$



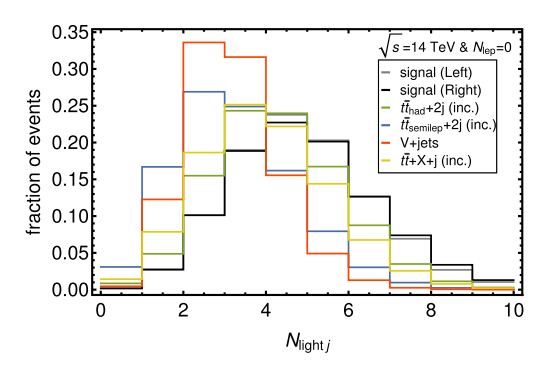


FIG. 2. Distributions (with $N_{\ell} = 0$) of the fraction of N_h (left panel) and N_i (right panel) for signal and background.

 $(h \to b\bar{b}), \ t\bar{t}_{\text{semilep}} + (\gamma^* \to b\bar{b}), \ t\bar{t}_{\text{had}} + (W \to l\nu),$ $t\bar{t}_{had} + (Z \to \nu\nu)$, and $t\bar{t}_{semilep} + (Z \to b\bar{b})$ are considered with one extra jet to each process, which leads to 2.9×10^3 expected events in this category.

- (5) V + jets production (V = Z or W). A b-jet pair and a light-jet pair leading to four extra jets and a genuine source of E_T^{miss} through neutrinos coming from the gauge boson decays [with BR($Z \rightarrow \nu \nu$) = 0.2 and BR($W \to l\nu$) = 0.21]. For $\mathcal{L} = 1000 \text{ fb}^{-1}$, 5.6×10^4 events for Z + jets and 3×10^5 events for W + jets are expected.
- (6) Diboson production. It is subdominant, with $\sim 10^{-3}$ times the V + jets number of events (which we will keep under control). Therefore, one can safely neglect this background.

In what follows, we will characterize the signal against the dominant SM backgrounds, which will allow us to find signal regions suitable for our search strategy. In the collider study to be developed, the backgrounds we have just defined fall into four categories: $t\bar{t}_{had} + 2j$ and $t\bar{t}_{\text{semilep}} + 2j$ (both inclusive), V + jets, and $t\bar{t} + X + j$ (also inclusive).

Distributions of the fraction of the number of identified b jets N_b , and the number of light jets N_i for the signal and the main backgrounds, are depicted in Fig. 2 (left and right panels, respectively). We consider the generic squark masses of 1 TeV for both the Left and Right production cases. First, a lepton veto $(N_{\ell} = 0)$ is set (already imposed on Fig. 2) in order to reduce the semileptonic $t\bar{t}$ production, which is one of the most dangerous backgrounds. It is important to note that the maximum of the N_i distribution for the signal is found for four light jets, while most of the backgrounds are chopped for a lower value of the light-jet multiplicity. In addition, the fact of having four bottom quarks coming from the two Higgs-boson decays is a challenging task, since in principle one wants to identify the four b jets. All of this motivates, on the one hand, the requirement of at least four light jets in our search strategy and, on the other hand, the definition of two signal regions: a first signal region (SR1) requiring at least four b jets in the final state, and a second one (SR2) with at least three identified b jets.

Figure 3 is devoted to the usual distributions—in particular, those related to the missing transverse energy E_T^{miss} . The missing energy distributions for the backgrounds have peaks below 100 GeV, while the signal has most of its events above this value.

Furthermore, the $E_T^{\rm miss}$ significance distributions of signal and background present different patterns with a clear separation near 5 GeV^{1/2}. The $\Delta \phi(j_1, \vec{p}_T^{\text{miss}})$ distributions show a noncentral behavior for signal and most of the irreducible backgrounds, but this variable is useful in order to reject most of the QCD multijet background. Following the data-driven analysis of this background in Ref. [24], we will include a conservative estimate of 0.7 events as the final number for the multijet background in the cut flow for $\mathcal{L} = 1000 \text{ fb}^{-1}$ (corresponding to a direct extrapolation from $\mathcal{L} = 139 \text{ fb}^{-1}$ to the luminosity considered here in the signal regions with at least four jets).

Finally, the $m_{\rm eff}$ variable is constructed as the sum of the missing transverse energy and the scalar sum of the transverse momenta of all the reconstructed jets (H_T) . The corresponding distributions of the background events have peaks below 1000 GeV, while the signal peak is near this value.

The distributions for both signal cases, *Left* (gray lines) and Right (black lines), are slightly different, but the general conclusions and the resulting cuts can be joined in order to get a less model-dependent search strategy.

Taking all this into account, the definition of the SR1 search strategy contains the cuts listed below:

- (1) Selection cuts $N_b \ge 4$, $N_j \ge 4$, $N_\ell = 0$. (2) χ_{HH}^2 cut lower than 2.

¹The $t\bar{t} + b\bar{b}$ with the extra b pair coming from a gluon was simulated with 47.5×10^3 expected events after generator cuts. However, the strong MET cut that we apply in the following search cancels all these events, and we then demand a genuine source of missing energy yielding to the described processes for this category and omit the $t\bar{t} + b\bar{b}$ process from now on.

²Following the definition in Ref. [25], this variable quantifies the requirement of two reconstructed bottom pairs coming from the Higgs bosons.

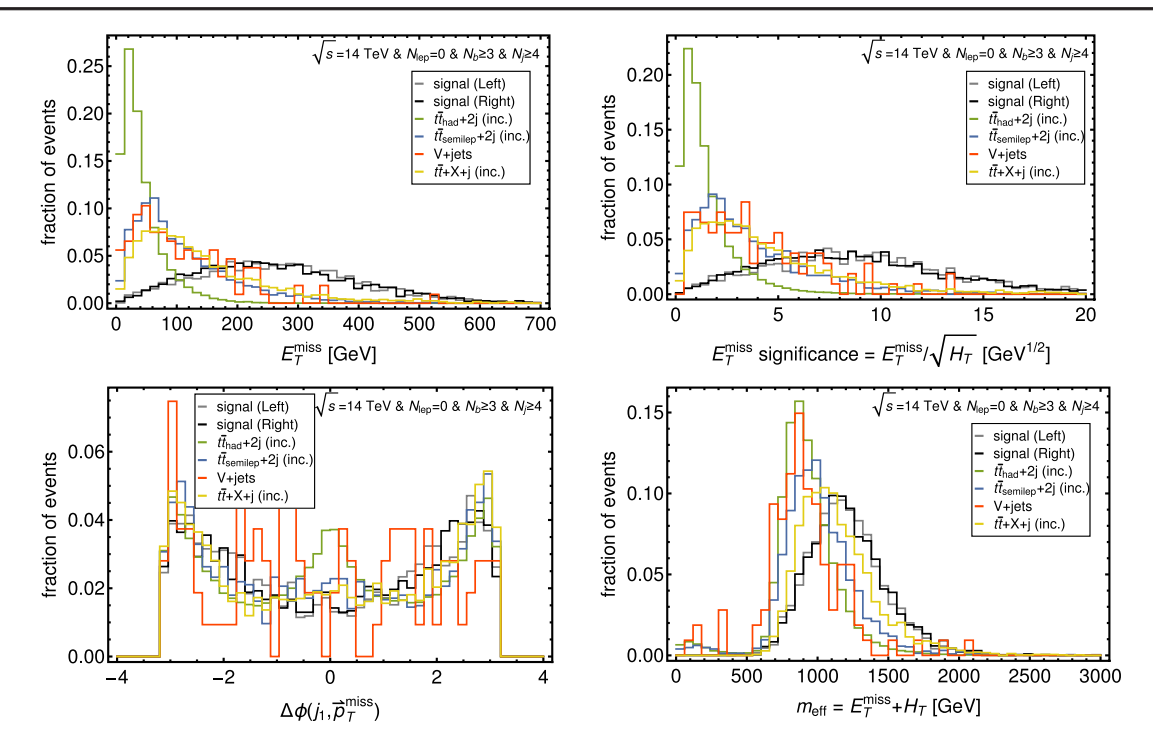


FIG. 3. Distributions (with $N_\ell=0$, at least three b jets, and four light jets) of the fraction of E_T^{miss} (upper-left panel), the E_T^{miss} significance (upper-right panel), the azimuthal angle difference $\Delta\phi(j_1,\vec{p}_T^{\text{miss}})$ between the leading jet and the \vec{p}_T^{miss} (lower-left panel), and the effective mass m_{eff} (lower-right panel), for signal and background.

- (3) MET cuts given by $E_T^{\text{miss}} > 150 \text{ GeV}$, $|\Delta \phi(j_1, \vec{p}_T^{\text{miss}})| > 0.4$, and $m_{\text{eff}} > 1300 \text{ GeV}$. Meanwhile, the search strategy for the signal region SR2 is defined with the following cuts:
 - (1) Selection cuts $N_b \ge 3$, $N_i \ge 4$, $N_{\ell} = 0$.
 - (2) p_T cuts of Eq. (2):

$$p_T^{j_1} > 200 \text{ GeV}, \qquad p_T^{j_2} > 150 \text{ GeV}, \qquad p_T^{j_3} > 80 \text{ GeV}, \qquad p_T^{j_4} > 40 \text{ GeV},$$

 $p_T^{b_1} > 100 \text{ GeV}, \qquad p_T^{b_2} > 60 \text{ GeV}, \qquad p_T^{b_3} > 35 \text{ GeV}.$ (2)

(3) MET cuts given by $E_T^{\text{miss}} > 150 \text{ GeV}$, $|\Delta \phi(j_1, \vec{p}_T^{\text{miss}})| > 0.4$, and $m_{\text{eff}} > 1400 \text{ GeV}$. For the statistical analysis, we consider the significance, including background systematic uncertainties [26,27], given by

$$S = \sqrt{2\left((B+S)\log\left(\frac{(S+B)(B+\sigma_B^2)}{B^2+(S+B)\sigma_B^2}\right) - \frac{B^2}{\sigma_B^2}\log\left(1 + \frac{\sigma_B^2 S}{B(B+\sigma_B^2)}\right)\right)},$$
(3)

where S (B) is the number of signal (background) events, and $\sigma_B = (\Delta B)B$, with ΔB being the relative systematic uncertainty chosen to be a conservative value of 30%. This conservative value takes the uncertainty associated with our limited statistics into account, since we mostly suppress the expected backgrounds by means of the use of our search strategy, as shown in the next section.

III. RESULTS

The cut-by-cut resulting significances with systematic uncertainties of 30%, with our search strategy applied to each signal region (SR1, SR2) and to *Left*, *Right* productions, are summarized in Tables I–IV. Remember that the search strategy was developed for $\mathcal{L}=1000~\mathrm{fb^{-1}}$, and a QCD multijet estimate of 0.7 events [24] was included in the significances of the last cut.

As we can see, most of the backgrounds were eliminated, and we keep at least five signal events at the end of the strategies. In particular, the results for SR1 in which we demand four reconstructed *b* jets, corresponding to the *Left* and *Right* productions, are collected in Tables I and II,

respectively. For each kind of signal, we expect significances of 3.16σ and 2.74σ for $\mathcal{L}=1000$ fb⁻¹. Even results at $\mathcal{L}=300$ fb⁻¹ are interesting with significances near 2σ . On the other hand, Tables III and IV show the results for the *Left* and *Right* productions in SR2 (in which we demand

TABLE I. Cut flow for SR1 with $\mathcal{L} = 1000 \text{ fb}^{-1}$ for the *Left* case signal production. Significances are from Eq. (3), with a systematic uncertainty in the background of 30%. A QCD multijet estimate of 0.7 events [24] is taken into account for the significances of the last cut-flow step.

Process	Signal	$t\bar{t}_{\rm had} + 2j$ (inc.)	$t\bar{t}_{\text{semilep}} + 2j \text{ (inc.)}$	V + jets	$t\bar{t}X + j$ (inc.)	S
Expected	2110	2.4×10^{6}	0.74×10^{6}	3.56×10^{5}	2.9×10^{3}	2×10^{-3}
Selection cuts	173.1	2697	90.2	7.95	13.2	1.3×10^{-2}
χ_{HH} cut	38.6	364.8	12.7	0	1.7	0.32
MET and $m_{\rm eff}$ cuts	6.9	1.1	0	0	0.1	3.16
$\mathcal{L}=300~\text{fb}^{-1}$	2.1	0.3	0	0	0	1.89

TABLE II. Cut flow for SR1 with $\mathcal{L} = 1000 \text{ fb}^{-1}$ for the *Right* case signal production. Significances are from Eq. (3), with a systematic uncertainty in the background of 30%. A QCD multijet estimate of 0.7 events [24] is taken into account for the significances of the last cut-flow step.

Process	Signal	$t\bar{t}_{\rm had} + 2j$ (inc.)	$t\bar{t}_{\text{semilep}} + 2j \text{ (inc.)}$	V + jets	$t\bar{t}X + j$ (inc.)	\mathcal{S}
Expected	1701	2.4×10^{6}	0.74×10^{6}	3.56×10^{5}	2.9×10^{3}	1.6×10^{-3}
Selection cuts	136.7	2697	90.2	7.95	13.2	0.16
χ_{HH} cut	31.9	364.8	12.7	0	1.7	0.27
MET and $m_{\rm eff}$ cuts	5.7	1.1	0	0	0.1	2.74
$\mathcal{L}=300~\text{fb}^{-1}$	1.72	0.3	0	0	0	1.63

TABLE III. Cut flow for SR2 with $\mathcal{L} = 1000 \text{ fb}^{-1}$ for the *Left* case signal production. Significances are from Eq. (3), with a systematic uncertainty in the background of 30%. A QCD multijet estimate of 0.7 events [24] is taken into account for the significances of the last cut-flow step.

Process	Signal	$t\bar{t}_{\rm had} + 2j$ (inc.)	$t\bar{t}_{\text{semilep}} + 2j \text{ (inc.)}$	V + jets	$t\overline{t}X + j$ (inc.)	$\mathcal S$
Expected	2110	2.4×10^{6}	0.74×10^{6}	3.56×10^{5}	2.9×10^{3}	2×10^{-3}
Selection cuts	616.9	3.06×10^{4}	2025	145.7	94.1	0.06
p_T cuts	35.9	216.7	4.1	0	2.1	0.49
MET and $m_{\rm eff}$ cuts	16.8	0	0.3	0	0.0	7.22
$\mathcal{L} = 300 \text{fb}^{-1}$	5	0	0.1	0	0	4.32

TABLE IV. Cut flow for SR2 with $\mathcal{L} = 1000 \text{ fb}^{-1}$ for the *Right* case signal production. Significances are from Eq. (3), with a systematic uncertainty in the background of 30%. A QCD multijet estimate of 0.7 events [24] is taken into account for the significances of the last cut-flow step.

Process	Signal	$t\bar{t}_{\rm had} + 2j$ (inc.)	$t\bar{t}_{\text{semilep}} + 2j \text{ (inc.)}$	V + jets	$t\bar{t}X + j$ (inc.)	\mathcal{S}
Expected	1701	2.4×10^{6}	0.74×10^{6}	3.56×10^{5}	2.9×10^{3}	1.6×10^{-3}
Selection cuts	508.9	3.06×10^{4}	2025	145.7	94.1	0.05
p_T cuts	38.3	216.7	4.1	0	2.1	0.05
MET and $m_{\rm eff}$ cuts	18.1	0	0.3	0	0.0	7.58
$\mathcal{L}=300~\text{fb}^{-1}$	5.4	0	0.1	0	0	4.55

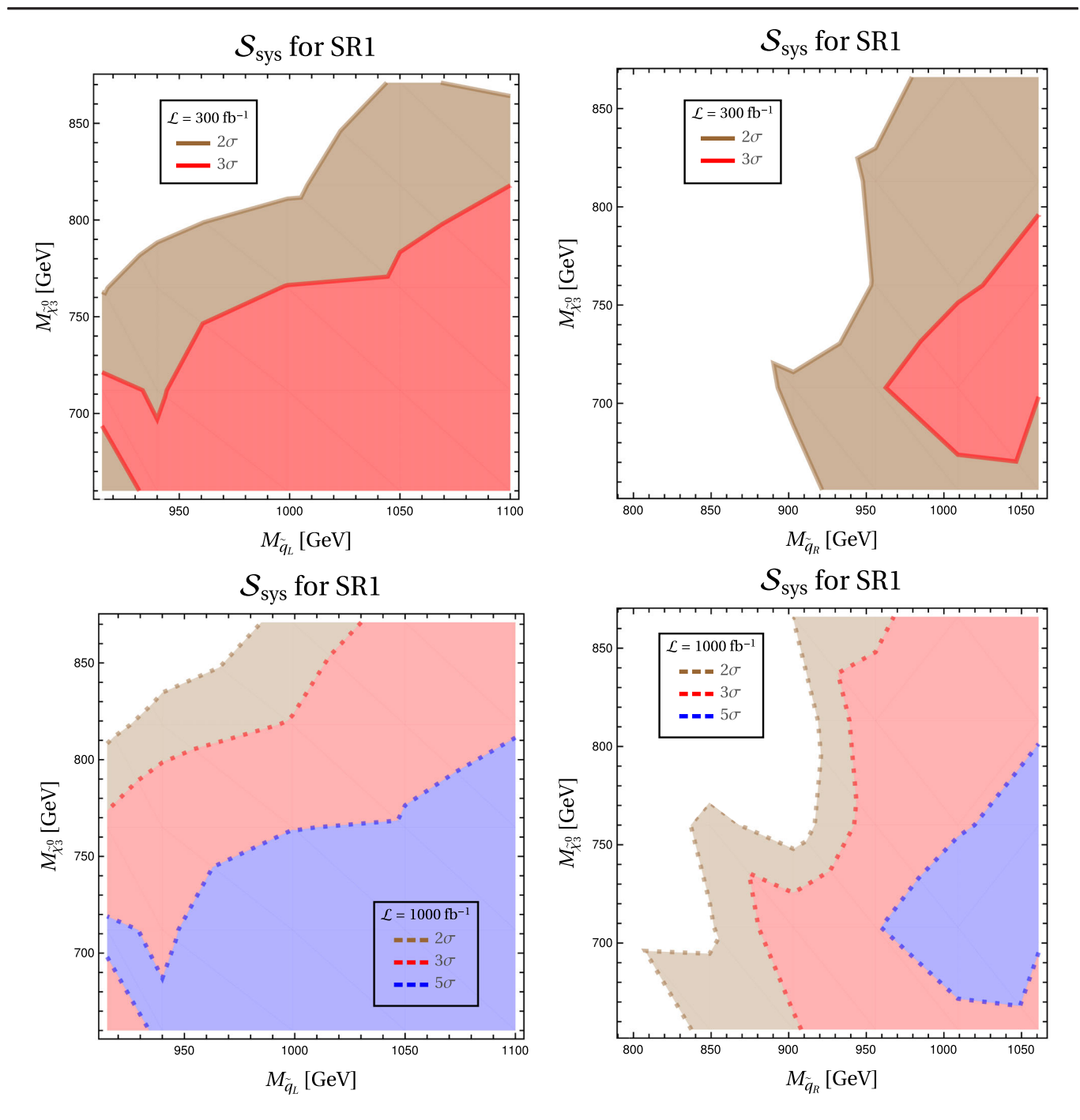


FIG. 4. Contour lines for SR1 in the plane $[M_{\tilde{q}}, M_{\tilde{\chi}_3^0}]$ corresponding to the \tilde{q}_L (*Left*) and \tilde{u}_R (*Right*) productions. The brown, red, and blue regions are the \mathcal{S} (background systematic uncertainty of 30%) with values of at least 2σ , 3σ , and 5σ , respectively. The upper (lower) panels correspond to $\mathcal{L} = 300 \, (1000) \, \mathrm{fb}^{-1}$.

three reconstructed b jets). Then, for this signal region, the results are very promising, with significances above 4σ (7 σ) for a luminosity of 300 (1000) fb⁻¹.

The search strategy exploits the large amount of $E_T^{\rm miss}$ and p_T of the several energetic b and light jets, which are very characteristic for the spectrum that we are considering —i.e., with the Higgsino LSP coming from an intermediate

bino state. Hence, we apply this general search strategy in order to study the sensitivity in the plane $[M_{\tilde{q}}, M_{\tilde{\chi}^0_3}]$, corresponding to the relevant parameters of these SUSY scenarios in which we fix the LSP mass to 500 GeV and decouple the rest of the spectrum. In particular, we explore the ranges of interest $M_{\tilde{q}} \in [800, 1100]$ GeV and $M_{\tilde{\chi}^0_3} \in [600, 900]$ GeV. The contour lines of S for SR1

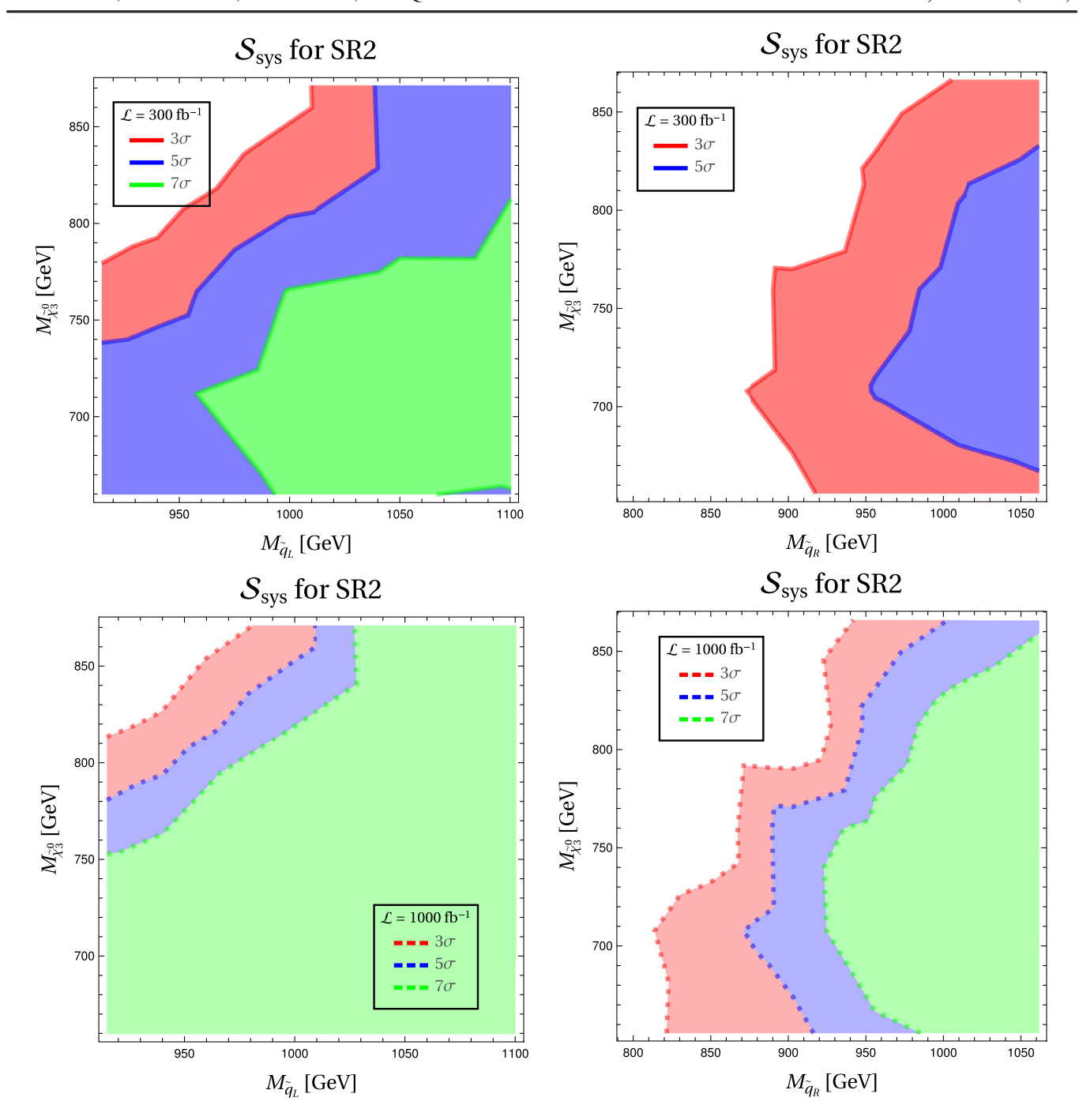


FIG. 5. Contour lines for SR2 in the plane $[M_{\tilde{q}}, M_{\tilde{\chi}_3^0}]$ corresponding to \tilde{q}_L (left) and \tilde{u}_R (right) productions. The red, blue, and green regions are the S (background systematic uncertainty of 30%) with values of at least 3σ , 5σ , and 7σ , respectively. Upper (lower) panels correspond to $\mathcal{L} = 300 \, (1000) \, \mathrm{fb}^{-1}$.

corresponding to the *Left* and *Right* productions are shown in Fig. 4. The upper and lower panels correspond to $\mathcal{L}=300$ and 1000 fb⁻¹, respectively, and the brown, red, and blue regions correspond to values of \mathcal{S} of at least 2σ , 3σ , and 5σ , respectively. With a luminosity of 300 fb⁻¹, we obtain significances at the evidence level in most of the region for $M_{\tilde{q}_L} \gtrsim 950$ GeV and $M_{\tilde{\chi}_3^0} \lesssim 750$ GeV in the *Left*

case. However, this region is reduced in the *Right* case. Notice that the projections to $\mathcal{L}=1000~\text{fb}^{-1}$ with discovery-level significance are very similar to the previous ones in both cases.

For SR2 in Fig. 5, we also include the green regions corresponding to significances of at least 7σ , since the results are improved with respect to the SR1 ones. We

expect more signal events after the cuts of this search strategy, and discovery-level significances arise even for $\mathcal{L}=300~{\rm fb^{-1}}$. In particular, we have $\mathcal{S}\geq 5\sigma$ for $M_{\tilde{q}_L}\gtrsim 950~{\rm GeV}$ and $M_{\tilde{\chi}_3^0}\lesssim 750~{\rm GeV}$ in the *Left* case, and $M_{\tilde{q}_R}\gtrsim 1000~{\rm GeV}$ and $700~{\rm GeV}\lesssim M_{\tilde{\chi}_3^0}\lesssim 800~{\rm GeV}$ for the *Right* case. It is not superfluous to again reiterate here that the parameter space of interest of these SUSY scenarios is not excluded by any of the experimental searches carried out at the LHC by the ATLAS and CMS Collaborations, as we have checked using CheckMATE. Therefore, with the very promising results obtained for LHC sensitivity, with both search strategies, we think that it would be interesting to develop experimental analyses of these channels starting from the signal interpretation that we propose.

IV. BRIEF DISCUSSION

Some comments are in order to summarize the main conclusions of this work. When one deviates from the assumption of 100% branching fractions of supersymmetric decays to the LSP, the current searches have a different interpretation. In this paper, we have analyzed a particular spectrum such that the mass of the first two squark generations is heavier than a mostly bino neutralino $(\tilde{\chi}_3^0)$, which in turn is heavier than a mostly Higgsino set of states $(\tilde{\chi}_{1,2}^0, \tilde{\chi}_1^+)$. Pair production of squarks at the LHC will generate a cascade decay via $\tilde{\chi}_3^0$, since the direct decay to the LSP is Yukawa suppressed.

We have first shown that, for the values of the masses considered along this work, the current LHC searches provide no bounds. Then we have studied the feasibility of discovery of this signal with two light jets, four b quarks and MET. The results are very promising, especially in the SR2 case, where one can even obtain 7σ significances for 300 fb⁻¹, within regions of the parameter space of the doublet case. The general message we want to convey is that one needs to deviate from simplified models to be able to cover a wide range of the parameter space in this class of BSM scenarios.

ACKNOWLEDGMENTS

The work of E.A. is partially supported by the "Atracción de Talento" program (Modalidad 1) of the Comunidad de Madrid (Spain) under Grant No. 2019-T1/TIC-14019, by the Spanish Research Agency (Agencia Estatal de Investigación) through the IFT Centro de Excelencia Severo Ochoa, Grant No. SEV-2016-0597, and by CONICET and ANPCyT (Argentina) under Projects No. PICT 2016-0164, No. PICT 2017-2751, and No. PICT 2017-2765. The work of A. D. was partially supported by the National Science Foundation under Grant No. PHY-2112540. The work of R. M. was supported by CONICET (Argentina). The work of M.Q. is partly supported by Spanish MINEICO under

No. FPA2017-88915-P, by the Catalan Government under Grant No. 2017SGR1069, and by Severo Ochoa Excellence Program of MINEICO under Grant No. SEV-2016-0588. IFAE is partially funded by the CERCA program of the Generalitat de Catalunya.

APPENDIX: DETAILS OF THE BENCHMARK POINTS

For each benchmark point generated with SOFTSUSY.4.1.10, we compute the expected signal event $S_{\rm exp}$ corresponding to the process $pp \to \tilde{q} \; \tilde{q} \to 2j + 4b + E_T^{\rm miss}$ to a given luminosity ${\cal L}$ by

$$S_{\text{exp}} = \sigma(pp \to \tilde{q} \, \tilde{q})$$

$$\times (\text{BR}(\tilde{q} \to q\tilde{\chi}_3^0) \text{BR}(\tilde{\chi}_3^0 \to \tilde{\chi}_{1,2}^0 h) \text{BR}(h \to b\bar{b}))^2$$

$$\times \mathcal{L}. \tag{A1}$$

We summarize in Tables V and VI the $\sigma \times BR$ values for the *Left* and *Right* cases, respectively.

In addition, the SUSY-breaking input parameters provided to SOFTSUSY.4.1.10 in order to generate the benchmark point corresponding to $M_{\tilde{\chi}_0^0}=818$ GeV and $M_{\tilde{q}_L}=1000$ GeV in Table V are (all masses are in TeV and at the $\mu=m_Z$ scale): $M_1=0.75,~M_2=3,~M_3=2.2,~A_t=A_b=A_\tau=0,~\mu=0.5,~m_A=8,~m_{\tilde{l}_L}=m_{\tilde{l}_R}=10$ $(l=e,~\mu,~\tau),~m_{\tilde{q}_{L1}}=0.955,~m_{\tilde{q}_{L2}}=m_{\tilde{q}_{L3}}=10,~M_{\tilde{d}_R}=15, M_{\tilde{d}_R}=10~(q=u,c,t,s,b),$ and $t_\beta=10$. The resulting

TABLE V. Values of $\sigma \times BR$ [fb] for each benchmark point in the $[M_{\tilde{q}}, M_{\tilde{z}_{1}^{0}}]$ plane of the *Left* case.

		$M_{ ilde{q}_L}$ [GeV]					
$M_{\tilde{\chi}^0_3}$ [GeV]	915	925	940	1000	1050	1100	
660	4.207	3.917	3.582	2.413	1.746	1.269	
712	4.515	4.216	3.934	2.727	2.000	1.469	
765	3.642	3.491	3.368	2.500	1.888	1.414	
818	2.008	2.107	2.265	2.035	1.645	1.283	
871	0.259	0.445	0.747	1.306	1.265	1.083	

TABLE VI. Values of $\sigma \times BR$ [fb] for each benchmark point in the $[M_{\tilde{q}}, M_{\tilde{\chi}^0_3}]$ plane of the *Right* case. For the (x) benchmark points, the $\tilde{u}_R \to u\tilde{\chi}^0_3$ channel is kinematically closed.

			$M_{ ilde{q}_R}$	[GeV]		
$M_{\tilde{\chi}^0_3}$ [GeV]	795	849	903	956	1009	1061
656	4.746	3.398	2.388	1.702	1.182	0.852
708	5.466	4.322	3.100	2.220	1.541	1.112
760	2.409	3.951	3.106	2.280	1.599	1.159
813	(x)	1.815	0.499	2.210	1.588	1.161
866	(x)	(x)	1.294	1.947	1.522	1.139

relevant branching ratios³ are BR($\tilde{d}_L \rightarrow d\tilde{\chi}_3^0$) = 0.75, BR($\tilde{u}_L \rightarrow u\tilde{\chi}_3^0$) = 0.74, BR($\tilde{\chi}_3^0 \rightarrow \tilde{\chi}_{1,2}^0 h$) = 0.26, and BR($h \rightarrow b\bar{b}$) = 0.57.

Finally, the SUSY-breaking input parameters provided to SOFTSUSY.4.1.10 in order to generate the benchmark point

- corresponding to $M_{\tilde{\chi}_3^0} = 813$ GeV and $M_{\tilde{q}_R} = 1009$ GeV in Table VI are as follows (all masses are in TeV and at the $\mu = m_Z$ scale): $M_1 = 0.75$, $M_2 = 3$, $M_3 = 2.2$, $A_t = A_b = A_\tau = 0$, $\mu = 0.5$, $m_A = 8$, $m_{\tilde{l}_L} = m_{\tilde{l}_R} = 10$ (l = e, μ , τ), $m_{\tilde{q}_{L1}} = m_{\tilde{q}_{L2}} = m_{\tilde{q}_{L3}} = 10$, $M_{\tilde{u}_R} = 1.1$, $M_{\tilde{q}_R} = 10$ (q = c, t, d, s, b), and $t_\beta = 10$. The resulting relevant branching ratios are $\mathrm{BR}(\tilde{d}_R \to d\tilde{\chi}_3^0) = 0.01$, $\mathrm{BR}(\tilde{u}_R \to u\tilde{\chi}_3^0) = 0.94$, $\mathrm{BR}(\tilde{\chi}_3^0 \to \tilde{\chi}_{1,2}^0 h) = 0.26$, and $\mathrm{BR}(h \to b\bar{b}) = 0.57$.
- [1] N. Arkani-Hamed, A. Delgado, and G. F. Giudice, The well-tempered neutralino, Nucl. Phys. **B741**, 108 (2006).
- [2] E. Arganda, A. Delgado, R. A. Morales, and M. Quirós, Novel Higgsino dark matter signal interpretation at the LHC, Phys. Rev. D 104, 055003 (2021).
- [3] E. Arganda, A. Delgado, R. A. Morales, and M. Quirós, Search strategy for gluinos at the LHC with a Higgs boson decaying into tau leptons, Eur. Phys. J. C 82, 971 (2022).
- [4] M. Guchait, A. Roy, and S. Sharma, Probing mild-tempered neutralino dark matter through top-squark production at the LHC, Phys. Rev. D 104, 055032 (2021).
- [5] A. Brignole, L. E. Ibanez, and C. Munoz, Soft supersymmetry breaking terms from supergravity and superstring models, Adv. Ser. Dir. High Energy Phys. 18, 125 (1998).
- [6] J. Alwall, R. Frederix, S. Frixione, V. Hirschi, F. Maltoni, O. Mattelaer, H.-S. Shao, T. Stelzer, P. Torrielli, and M. Zaro, The automated computation of tree-level and next-to-leading order differential cross sections, and their matching to parton shower simulations, J. High Energy Phys. 07 (2014) 079.
- [7] T. Sjöstrand, S. Ask, J. R. Christiansen, R. Corke, N. Desai, P. Ilten, S. Mrenna, S. Prestel, C. O. Rasmussen, and P. Z. Skands, An introduction to PYTHIA 8.2, Comput. Phys. Commun. 191, 159 (2015).
- [8] DELPHES 3 Collaboration, DELPHES 3, A modular framework for fast simulation of a generic collider experiment, J. High Energy Phys. 02 (2014) 057.
- [9] D. Dercks, N. Desai, J. S. Kim, K. Rolbiecki, J. Tattersall, and T. Weber, CheckMATE 2: From the model to the limit, Comput. Phys. Commun. 221, 383 (2017).
- [10] ATLAS Collaboration, Search for electroweak production of supersymmetric states in scenarios with compressed mass spectra at $\sqrt{s} = 13$ TeV with the ATLAS detector, Phys. Rev. D **97**, 052010 (2018).
- [11] CMS Collaboration, Search for Higgsinos decaying to two Higgs bosons and missing transverse momentum in proton-proton collisions at $\sqrt{s} = 13$ TeV, J. High Energy Phys. 05 (2022) 014.
- [12] ATLAS Collaboration, Search for supersymmetry in final states with missing transverse momentum and multiple b-jets in proton-proton collisions at $\sqrt{s} = 13$ TeV with the ATLAS detector, Report No. ATLAS-CONF-2018-041.

- [13] M. Mangano, The so-called MLM prescription for ME/PS matching, in *Proceedings of the Fermilab ME/MC Tuning Workshop* 2002, http://www-cpd.fnal.gov/personal/mrenna/tuning/nov2002/mlm.pdf.gz (2002).
- [14] M. L. Mangano, M. Moretti, F. Piccinini, and M. Treccani, Matching matrix elements and shower evolution for topquark production in hadronic collisions, J. High Energy Phys. 01 (2007) 013.
- [15] B. C. Allanach, SOFTSUSY: A program for calculating supersymmetric spectra, Comput. Phys. Commun. 143, 305 (2002).
- [16] B. C. Allanach and T. Cridge, The calculation of sparticle and Higgs decays in the minimal and next-to-minimal supersymmetric standard models: SOFTSUSY4.0, Comput. Phys. Commun. 220, 417 (2017).
- [17] B. C. Allanach, P. Athron, L. C. Tunstall, A. Voigt, and A. G. Williams, Next-to-minimal softsusy, Comput. Phys. Commun. **185**, 2322 (2014).
- [18] B. C. Allanach and M. A. Bernhardt, Including R-parity violation in the numerical computation of the spectrum of the minimal supersymmetric standard model: SOFTSUSY, Comput. Phys. Commun. 181, 232 (2010).
- [19] B. C. Allanach, C. H. Kom, and M. Hanussek, Computation of neutrino masses in R-parity violating supersymmetry: SOFTSUSY3.2, Comput. Phys. Commun. **183**, 785 (2012).
- [20] B. C. Allanach, A. Bednyakov, and R. Ruiz de Austri, Higher order corrections and unification in the minimal supersymmetric standard model: SOFTSUSY3.5, Comput. Phys. Commun. 189, 192 (2015).
- [21] B. C. Allanach, S. P. Martin, D. G. Robertson, and R. R. de Austri, The inclusion of two-loop SUSYQCD corrections to gluino and squark pole masses in the minimal and next-tominimal supersymmetric standard model: SOFTSUSY3.7, Comput. Phys. Commun. 219, 339 (2017).
- [22] C. Borschensky, Z. Gecse, M. Kraemer, R. van der Leeuw, A. Kulesza, M. Mangano et al., LHC SUSY Cross Section Working Group, https://twiki.cern.ch/twiki/bin/view/ LHCPhysics/SUSYCrossSections (2020).
- [23] W. Hollik, J. M. Lindert, and D. Pagani, NLO corrections to squark-squark production and decay at the LHC, J. High Energy Phys. 03 (2013) 139.
- [24] ATLAS Collaboration, Search for squarks and gluinos in final states with jets and missing transverse momentum

³Even though there is a splitting between the first and second generation of squarks, our spectrum is free from flavor constraints [28].

- using 139 fb⁻¹ of $\sqrt{s} = 13$ TeV pp collision data with the ATLAS detector, J. High Energy Phys. 02 (2021) 143.
- [25] ATLAS Collaboration, Search for pair production of Higgs bosons in the $b\bar{b}b\bar{b}$ final state using proton-proton collisions at $\sqrt{s}=13$ TeV with the ATLAS detector, J. High Energy Phys. 01 (2019) 030.
- [26] G. Cowan, K. Cranmer, E. Gross, and O. Vitells, Asymptotic formulae for likelihood-based tests of new physics, Eur. Phys. J. C 71, 1554 (2011).
- [27] G. Cowan, Discovery sensitivity for a counting experiment with background uncertainty, Technical Report (Royal Holloway, London, 2012) http://www.pp.rhul.ac.uk/~cowan/stat/medsig/medsigNote.pdf.
- [28] K. Blum, Y. Grossman, Y. Nir, and G. Perez, Combining $K^0 \bar{K}^0$ Mixing and $D^0 \bar{D}^0$ Mixing to Constrain the Flavor Structure of New Physics, Phys. Rev. Lett. **102**, 211802 (2009).